www.czasopisma.pan.pl PAN POLSKA AKADEMIA NAUK www.journals.pan.pl

Arch. Metall. Mater. **63** (2018), 4, 1875-1881

DOI: 10.24425/amm.2018.125118

F. RADKOVSKÝ*#, M. GEBAUER**#, V. MERTA*

OPTIMIZING OF METAL FOAM DESIGN FOR THE USE AS A HEAT EXCHANGER

The work deals with possibilities of using this specific material. It is focused on cast metal foams with a regular arrangement of internal cells and it refers to already used casting technologies – the production of metal foamswith the aid of sand cores. Metal foamsare used in many industries, such as: automotive, aerospace, construction, power engineering. They have unique propertiesand due to lower weight with sufficient strength and greater contact surface can be used, for example, for the conduction of heat. This article deals with the useof the metal foam as a heat exchanger. The efficiency of the heat exchanger depends on its shape and size and therefore the study is focused first on the optimization of the shape before the proper manufacture.

Keywords: metal foam; 3D modeling; heat exchanger; heat conduction; efficiency

1. Introduction

The metal foam can be described as a material of the future – technologies of its production in order to take advantage of its full application potential are still being developed at present. The metal foam is a material that contains in its structure the intentionally created pores, thanks to which it then stands out for its many unique properties. The most important of them is the low specific weight while maintaining sufficient strength. Metal foams that are discussed in this contribution are made by conventional foundry process, and namely by infiltration of liquid metal into the mould cavity filled with a complex core – a preform. Fig. 1 shows a foundry core assembled of six stages. Using these processes a metal foam with regularly distributed and interconnected pores is obtained. Thanks to this it is possible to use the casting for flowing of gas or liquid medium, see Fig. 2. By changing the geometry of internal poresa greater contact surface is obtained and if the casting is divided on 2 parts with a solid wall it can be used as a heat exchanger. A method of computer simulation that will help to compare the designed geometries of the exchanger was chosen as a solution tool [1,2].

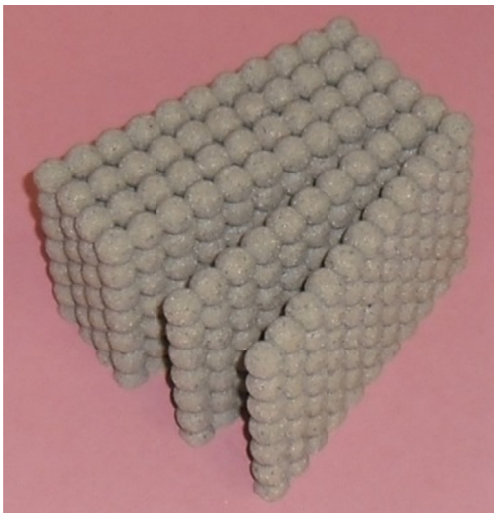

Fig. 1. Preform with cellular structure

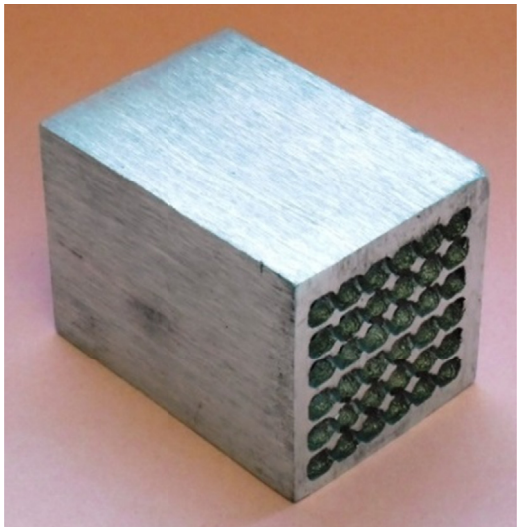

Fig. 2. Metal foam with regular structure

* VŠB-TECHNICAL UNIVERSITY OF OSTRAVA, FACULTY OF MATERIALS SCIENCE AND TECHNOLOGY, DEPARTMENT OF METALLURGY AND FOUNDRY ENGINEERING, 17. LISTOPADU 15/2172, OSTRAVA-PORUBA, CZECH REPUBLIC
** VŠB-TECHNICAL UNIVERSITY OF OSTRAVA, IT4INNOVATIONS, 17. LISTOPADU 15/2172, OSTRAVA-PORUBA, CZECH REPUBLIC
# Corresponding autors: filip.radkovsky@vsb.cz; marek.gebauer.@vsb.cz

2. Preparation of the experiment

Robust numerical methods of computer modeling, e.g. FEM, CFD etc., are put among the most powerful tools for designing the machinery or predictingthe future possible problems. These methods have been developed to minimize the amount of physical experiments that are lengthy and high expensive. With the help of computer modeling it is possible to virtually test a variety of variants of a particular component and then to choose the best solution, which is then subjected to experimental measurements and prototype testing [3].

Basic relations that are used for calculations of the finite volumes were implemented in the ANSYS CFX program. According to physical laws of the conservation of mass, momentum and energy interpreted by authors [4-6] we get the equations describing the flow of real fluids. For the simplified record of law equations that describes the fluid flow the so-called Einstein's summation rule is used. The equation of continuity expresses the law of conservation of mass, which has a form for non-stationary compressible fluids in a differential form (1). Where ρ [kg·m^{-3}] is the density of the liquid; t [s] the time; u_j [m·s^{-1}] velocity components; x_j [m] the spatial coordinates.

$$\frac{\partial \rho}{\partial t} + \nabla(\rho \cdot u) = 0 \tag{1}$$

The equation of the law of conservation of momentum is defined as the total change of momentum in a given volume of liquid and it is equal to the sum of all the forces acting on this volume (the sum of the volume and surface forces) [4]. According to the literature [5-6] its full text for a compressible medium has the form (2). Where p [Pa] is pressure; g_i [m·s^{-2}] gravitational constant; μ [m^2·s^{-1}] kinematic viscosity.

$$\rho \frac{Du}{Dt} = -\nabla p + \rho g + \mu \left[\nabla^2 u + \frac{1}{3} \nabla(\nabla \cdot u) \right] \tag{2}$$

Provided that the medium is incompressible $\nabla \cdot \mathrm{u} = 0$ from the equation(2) and we get the equation (3)

$$\rho \frac{Du}{Dt} = -\nabla p + \rho g + \mu \nabla^2 u \tag{3}$$

If the viscous effectsare negligible, we get so-called Euler's equation (4) [6]

$$\rho \frac{Du}{Dt} = -\nabla p + \rho g \tag{4}$$

In [5] it is possible to find also the form (5),which is actually the Navier-Stokes equation in Einstein notation.

$$\frac{\partial u_i}{\partial t} + \frac{\partial u_i u_j}{\partial x_j} = -\frac{1}{\rho} \frac{\partial p}{\partial x_i} + \nu \frac{\partial^2 u_i}{\partial x_j^{\,2}} + f_i \tag{5}$$

According to [4] the law of conservation of energy is defined as a total change of the fluid energy in a certain volume V and it is given by a change of internal energy, kinetic energy and the flow of both energies through the area S limiting the volume V. In most cases it is expressed with the aid of total enthalpy h_{tot} [m^2·s^{-2}], which is given by a sum of the static enthalpy and kinetic energy (6). Where λ [W·m·K^{-1}] is the thermal conductivity; T [K] thermodynamic temperature; τ [Pa] tensor of the shear stress.

$$\frac{\partial(\rho \cdot h_{tot})}{\partial t} + \frac{\partial(\rho \cdot u_j \cdot h_{tot})}{\partial x_j} - \frac{\partial p}{\partial t} = = \frac{\partial}{\partial x_j}\left(\lambda \cdot \frac{\partial T}{\partial x_j} \right) + \frac{\partial(u_j \cdot \tau_{jl})}{\partial x_l} + \rho \cdot f_j \cdot u_j \tag{6}$$

The basic laws of the conservation of mass, momentum and energy form a system of nonlinear partial equations for the variables p, u_i and h_{tot} or T. After adding the boundary conditions these equations are used for the solution of specific problems in fluid mechanics [4].

First we made a prototype of a possible heat exchanger as the metal foam with regular internal structure and a solid wall in the middle part. Based on this successful experiment the geometric models of the metal foam heat exchanger and classic tubular heat exchanger (geometry 1 to 7) were created. These variants were evaluated in the simulation software Ansys 16. As stated by the authors in the article [7] it has been calculated that the metal foam has a noticeably higher effect on heat transfer. Thanks to this positive result the next variants of different geometry were designed and they were calculated in the newly acquired programming environment of Ansys R18.0.

3. Proper experiment

This part of the work is devoted to the design and testing of geometries of the metal foam with regular internal arrangement for the use as a heat exchanger. 7 different geometries of cocurrent heat exchangers, which are shown in Fig. 3-9 were designed.

These are the heat exchangers with spherical nuclei, each different from each other either with different arrangement during casting or the inlets and outlets from them are adjusted. Mathematical models included the network in the range of 500-800 thousand cells depending on the specific geometry. Heat

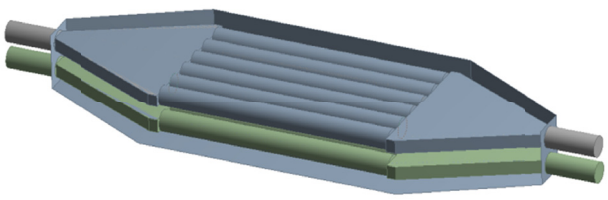

Fig. 3. Geometry 1

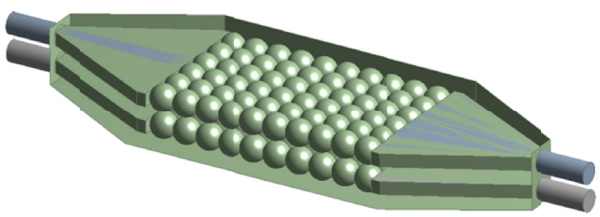

Fig. 4. Geometry 2

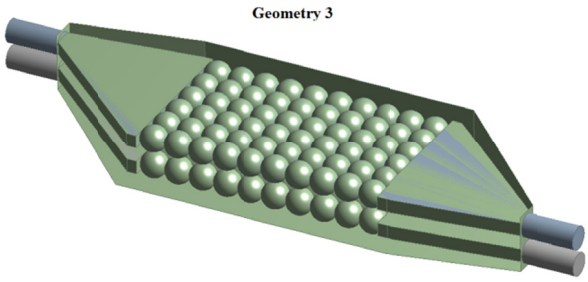

Fig. 5. Geometry 3

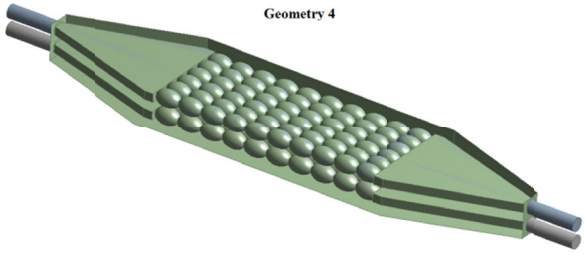

Fig. 6. Geometry 4

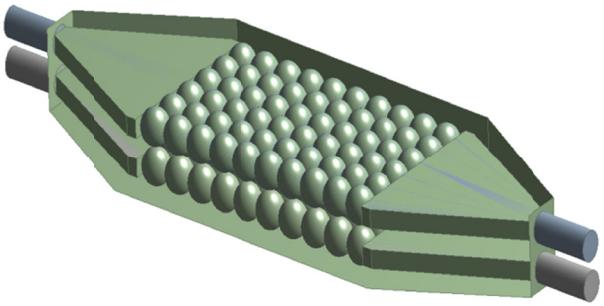

Fig. 7. Geometry 5

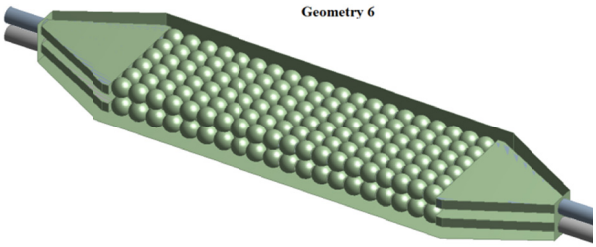

Fig. 8. Geometry 6

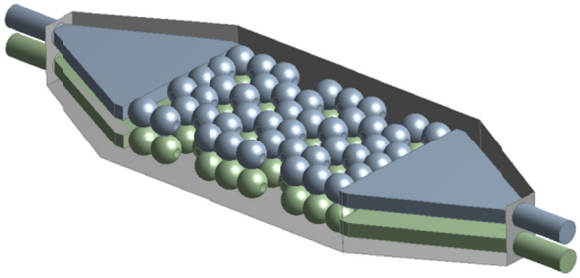

Fig. 9. Geometry 7

exchangers were simulated with the same boundary conditions on the inlet, outlet and on the wall for reasons of comparison of the results between them. A variant of the conventional tube heat exchanger and its outlets were chosen as a reference. The results are included in tables. Calculation of geometries was divided into two major domains. The first domain represented the running water inside the heat exchangers. The second domain represented a solid body representing a metal exchanger. Material properties of both domains are summarized in Table 1.

TABLE 1

Material properties

	Domain	
	Water	**Aluminium**
Thermal conductivity [W/mK]	0.6069	237
Specific heat capacity-cp [kg/JK]	4181	903
Density under 20 °C [kg/m^3]	997	2702
Dynamic viscosity [kg/ms]	8.9E-4	—

The roughness of walls is not included in the calculation. On the walls of the heat exchangers the heat transfer coefficient of the value of 5 Wm^{-2}K^{-1} was applied, which represents a body freely laid down in the space of cooling by natural convection [8]. For both inlets of the exchanger a condition of speed of the value 1 ms^{-1} is prescribed and at the outlet a condition of relative static pressure of the value 0 Pa is prescribed. However, for the upper stagea temperature boundary condition of the value of 80°C is prescribed and forthe bottom stage of the value 20°C is prescribed. Table 2 summarizes the initial values of boundary conditions.

TABLE 2

Boundary conditions

Inlet		**Outlet**	
The temperature of the upper floor [°C]	80	Average static pressure [Pa]	0
The temperature of the bottom floor [°C]	20	Average static pressure [Pa]	0
The flow velocity in the upper floor [m/s]	1		
The velocity in the bottom floor [m/s]	1		

Based on the calculation of the Reynolds number according to the relationship (7) a turbulent model of flowing *k*-*ω* SST was chosen, which is suitable for small Reynolds numbers up to about Re < 200 000.

$$\mathrm{Re} = \frac{v_s \cdot d}{\upsilon} = \frac{1 \cdot 0.008}{1.06 \cdot 10^{-6}} = 7547 \tag{7}$$

where v_s [m/s] is the mean velocity of the liquid flowing; d [m] the hydraulic diameter and υ [m^2/s] in our case the diameter of the tubes and the diameter of the kinematic viscosity. According to [4] if the value is Re < 2320 it is assumed the flow will have a laminar character; for 2320 < Re < 4000 the area of interest is the transition state between laminar and turbulent flowing; and Re > 4000 indicates the turbulent flow.

4. Results and discussion

The calculation was launched on a workstation with 16 CPus, 64GB Ram and SSD disk. Calculations lastedafter debugging the task about 2 days. The convergence criterion was set for all simulated heat exchangers to the accuracy of 2E-5. Imbalance of energies did not exceed the recommended value of error of 1%. For comparisingindividual models with each other the accuracy is sufficient. Temperature profile given in the lateral cross-section of the cooled stage is evaluated on the outlet of the studied area in the direction of the axis z. Fig. 10 shows this place marked with the red line. The resulting heat field is displayed in the section plane through the center of the spherical core of the cooled stage, see Fig. 11.

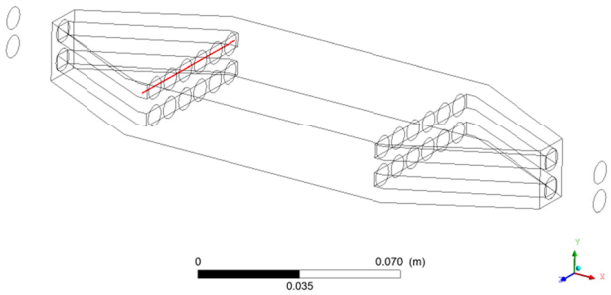

Fig. 10. Temperature profile in lateral cross-section

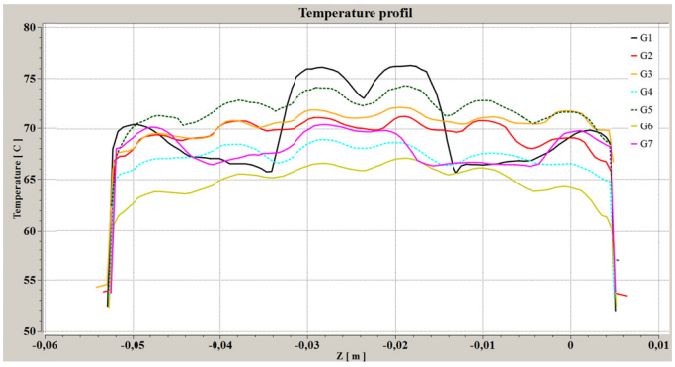

Fig. 11. Temperature profile in lateral cross-section

The results in table 3 include the average temperature at the outlet of heat exchangers of both stages. Values different towards specified values on the inlets (20°C and 80°C) are added in the table too. It is evident thatas a result of the planar symmetry the numeric values are the same, they differ with a sign only. For this reason the results are rendered only on the cooled side. For a better visibility the data are plotted in a chart, see Fig. 12.

TABLE 3

Summarizes the average values of the outlet areas of the forth heat exchangers

	Temperature [°C]		Difference [°C]	
	hot side	cold side	hot side	cold side
Geometry 1	74.35	25.65	–5.65	5.65
Geometry 2	68.85	31.15	–11.15	11.15
Geometry 3	69.75	30.25	–10.25	10.25
Geometry 4	66.45	33.45	–13.55	13.55
Geometry 5	71.65	28.35	–8.35	8.35
Geometry 6	64.65	35.35	–15.35	15.35
Geometry 7	68.65	31.35	–11.35	11,35

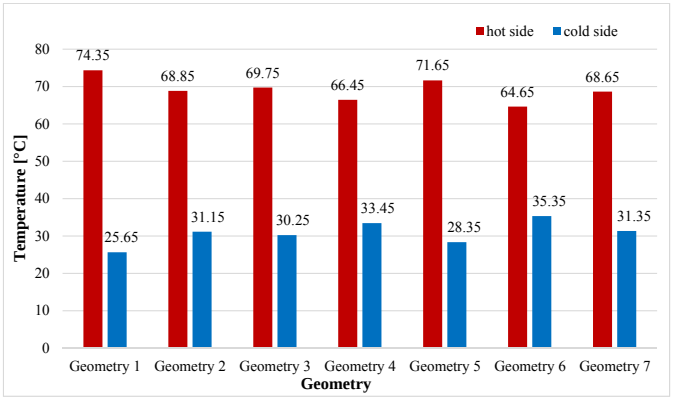

Fig. 12. Average temperature at the outlet from the both stages of the heat exchangers

In Fig. 13 shows a heat exchanger with the geometry No 1. According its results it finished the worst one of all the tested with regard to the temperature distribution. As it is evident from Table 3 and Fig. 12 its values are approximately 75°C at the outlet and it is characteristic with its uneven heat field in the transverse

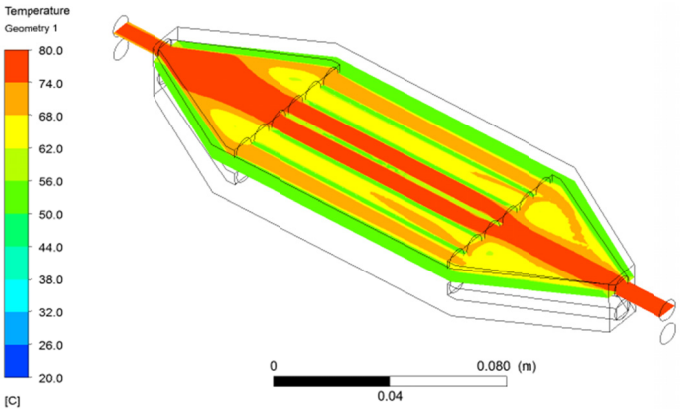

Fig. 13. Temperature profile in lateral cross-section (geometry 1)

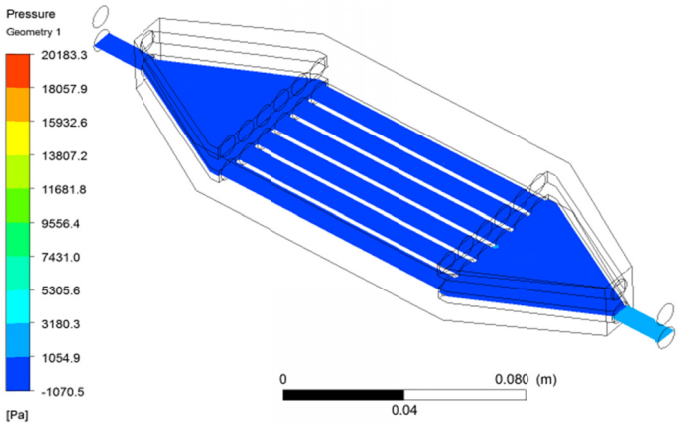

Fig. 14. Pressure profilein lateral cross-section (geometry 1)

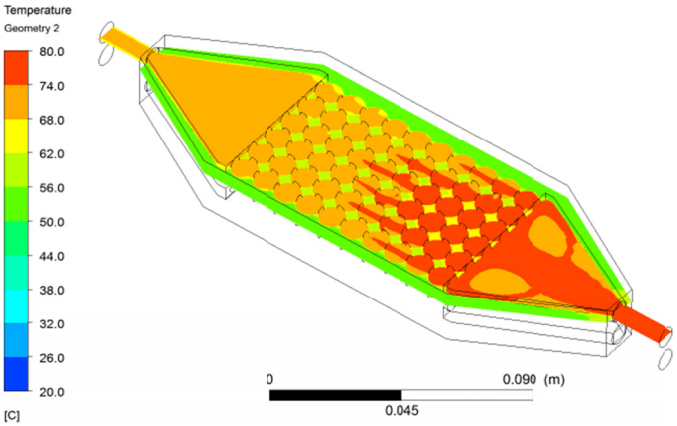

Fig. 15. Temperature profile in lateral cross-section (geometry 2)

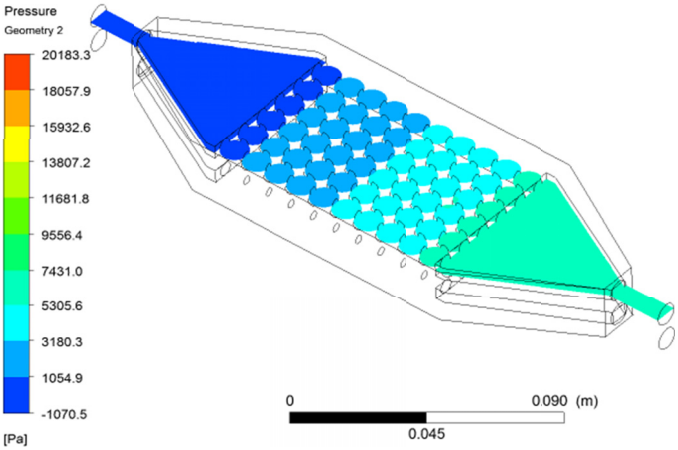

Fig. 16. Pressure profile in lateral cross-section (geometry 2)

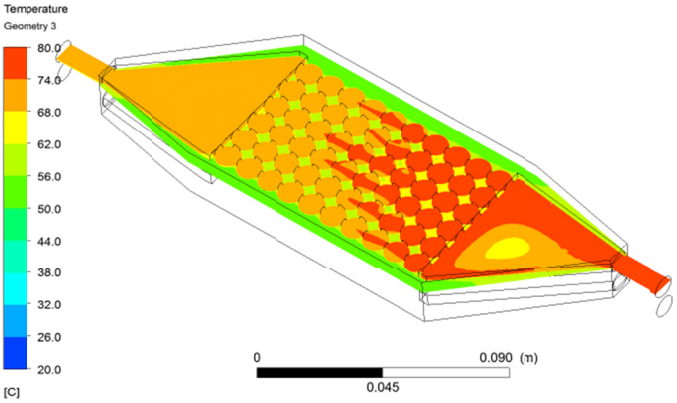

Fig. 17. Temperature profile in lateral cross-section (geometry 3)

direction. On the contrary it can be stated that its pressure field has the lowest and almost constant values throughout the entire cross-section of the heat exchanger, see Fig. 14. The geometry No 2 in Figs. 15 and 16 shows the average values. Heat distribution of the exchanger with geometry No 3 is similar to the geometry No 5. Its values at the outlet are approximately 70°C, which is only about two degrees lower than for the geometry No 5, see Figs. 17 and 21. On the contrary the pressure values at the inlet are about 5000 Pa higher, see Figs. 18 and 22. This type of the heat exchanger (geometry No 3) will not be realized

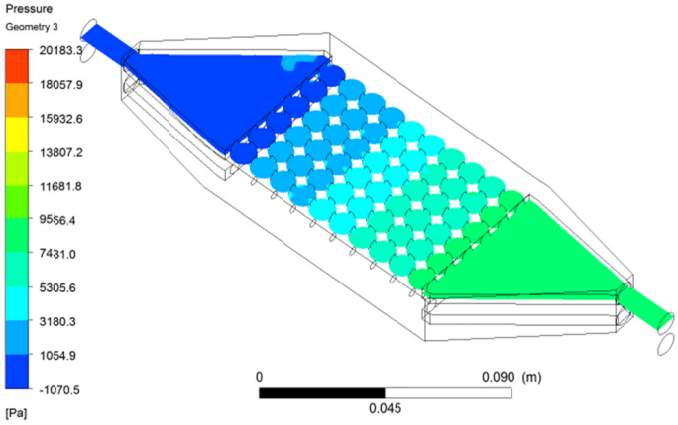

Fig. 18. Pressure profile in lateral cross-section (geometry 3)

too for the reasons of the overall production and savings of the pump parameters.

The heat exchanger with the geometry No 4 (see Figs 19 and 20) was considered the best option. Its elongated geometry shows, as the second one in the order, the highest heat transfer and low thermal gradient in the direction of liquid flowing. The temperature at the outlet is about 13°C lower than that of the reference exchanger. The production is not as complicated as it is in the case of the heat exchanger with geometry No 6. And for the required speed inlet no strong pump will be needed as in the case of the geometry No 7.

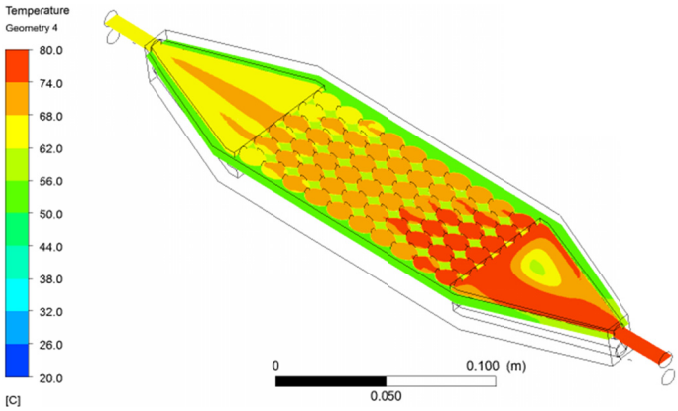

Fig. 19. Temperature profile in lateral cross-section (geometry 4)

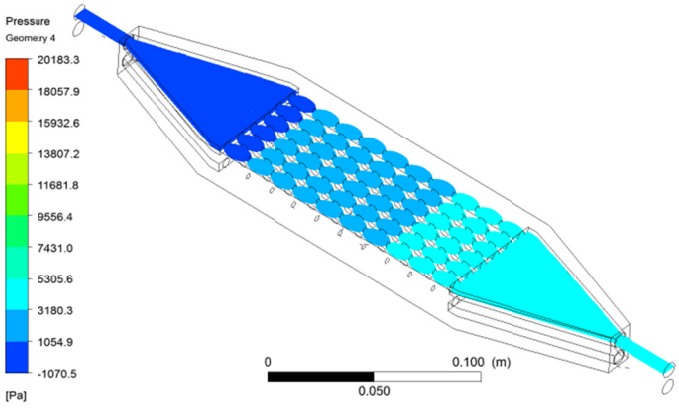

Fig. 20. Pressure profile in lateral cross-section (geometry 4)

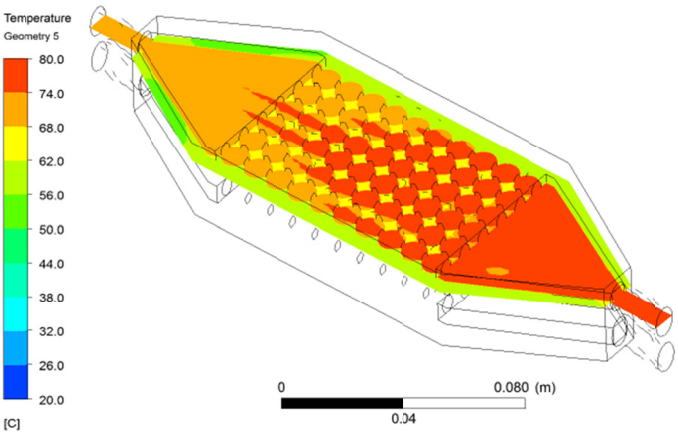

Fig. 21. Temperature profile in lateral cross-section (geometry 5)

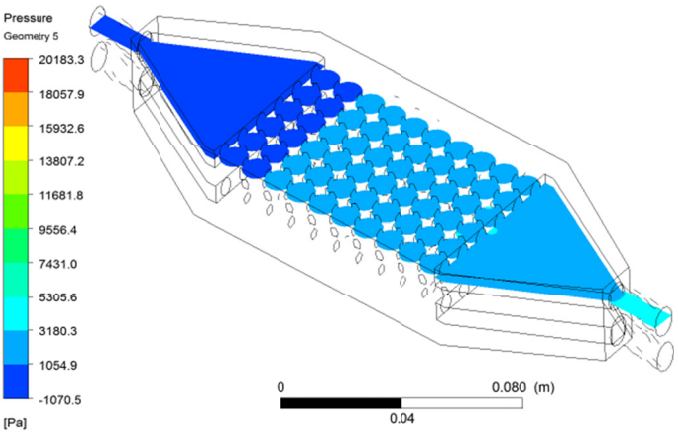

Fig. 22. Pressure profile in lateral cross-section (geometry 5)

By comparing the results of all heat exchangers, Figs. 13-26, it can be found out that the best results are achieved for the exchanger with the geometry No 6. Its temperature distribution is the smoothest one of all investigated types. At the outlet of the spherical area, Fig. 23, its values range from about 60°C to 66°C. It could the most effectively absorb the heat from the liquid, and so it helped to total cooling. Its maximum average temperature at the outlet is about 68°C, which is about 12°C less as compared to the reference heat exchanger with the geometry of No 1. However, this exchanger is twice bigger and heavier.

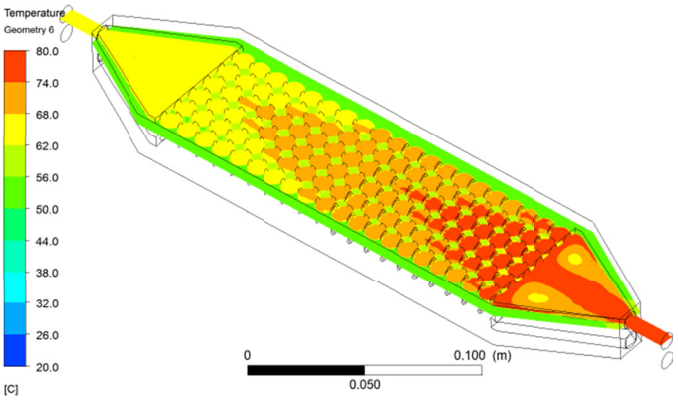

Fig. 23. Temperature profile in lateral cross-section (geometry 6)

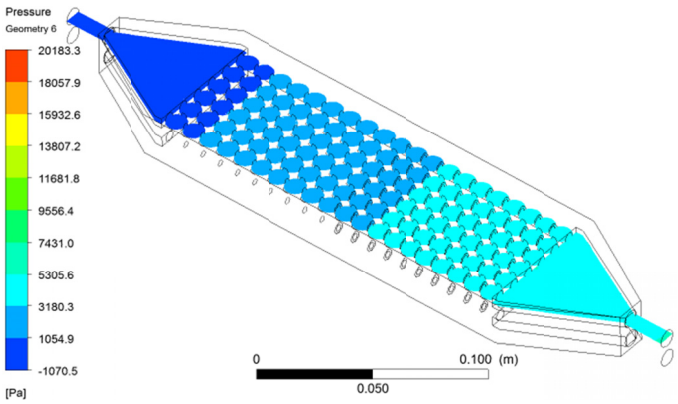

Fig. 24. Pressure profile in lateral cross-section (geometry 6)

Its production would be about 30% more expensive and the possibility of spoilage of 20% or more. If the temperature difference is compared with other geometries, it is proposed to consider if to realize this type of the long exchanger.

Figs. 25 and 26 show the heat exchanger with interrupted geometry No 7. Thermal values don't excel in any way over the others, but its pressure drop is the highest one from all the others. For the application in the industry it would be necessary to have a four times stronger pump in order to achieve the desired inlet boundary conditions (flow velocity 1 ms^{-1}). In addition, the production of this variant is financially the most demanding one.

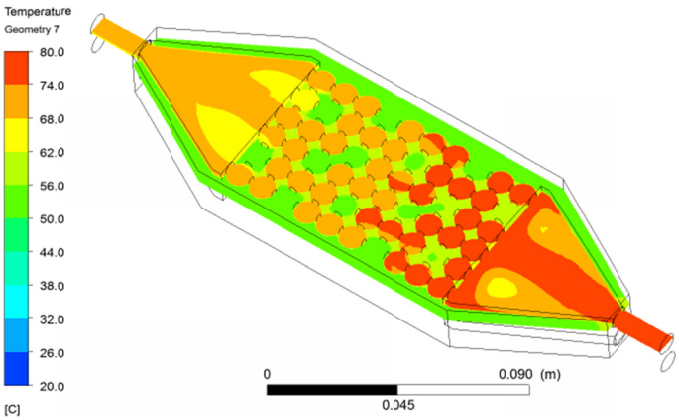

Fig. 25. Temperature profile in lateral cross-section (geometry 7)

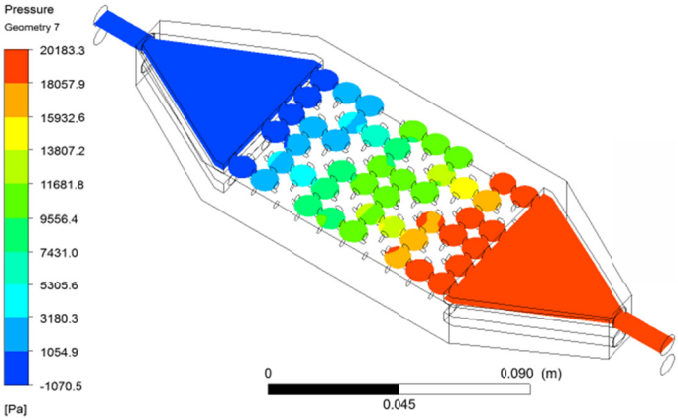

Fig. 26. Pressure profile in lateral cross-section (geometry 7)

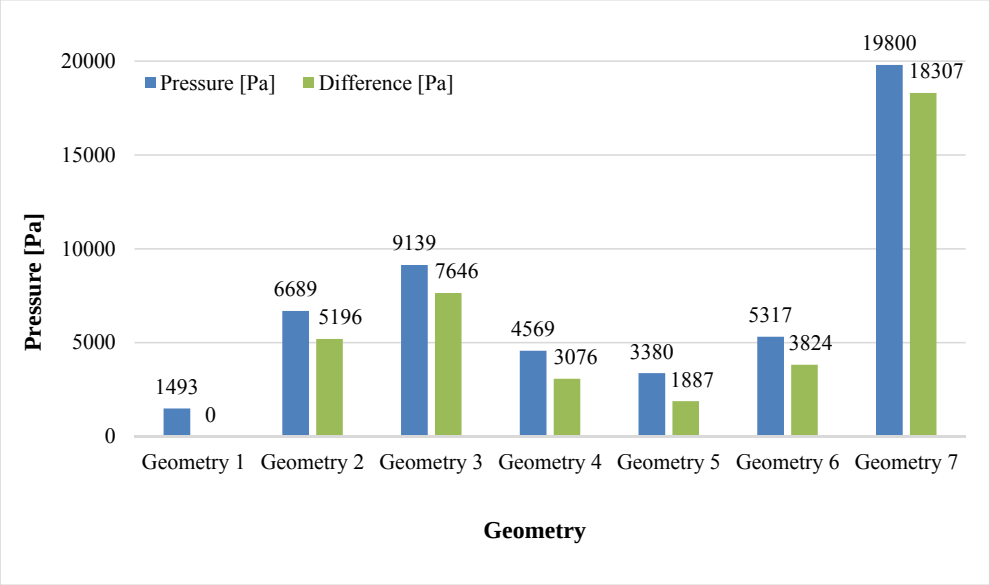

Fig. 27. Pressure values at the inlet from the both stages

Fig. 27 shows a comparison of the average relative pressure at the inlet from individual heat exchangers. The blue column indicates the readings and the green one is the difference to the reference heat exchanger with the geometry No 1.

5. Conclusions

Altogether seven types of heat exchangers with different geometry were simulated. The exchanger No 1 has the geometry of a conventional tube heat exchanger, which is used for the purposes of comparing the results with the so-called foam heat exchangers towards the reference. CFD simulation clarified the confusions about heat transfers, heat distribution and pressure drop.

It has been concluded that for a future real experiment some types will not be manufactured and subjected to the tests. The worst results showed the heat exchangers with the geometry No 6 and 7.

The number six has the highest efficiency of the heat transfer but in the context of its production and financial difficulty and weight the realization of the experiment is probably not worth.

The number seven showed the worst results as regards the pressure drop. In order to achieve the same inlet conditions it would be necessary to use a considerably more powerful pump than must be for the others, not to mention the technical feasibility.

The best parameters reached the geometry of the No 4. Its extended geometry showed the most effective heat transfer, inlet conditions can be realized with the aid of smaller pumps and technically it is easier to manufacture.

Acknowledgement

The paper was worked out with the financial support of Technology Agency of the Czech Republic(TA02011333 and TH02020668), project of "Student Grant Competition" numbers SP2018/77 and SP2018/60 and this work was supported by The Ministry of Education, Youth and Sports from the National Programme of Sustainability (NPU II) project "IT4 Innovations excellence inscience – LQ1602".

REFERENCES

[1] J. Banhart, Manufacture, characterisation and application of cellular metals and metal foams. Progress in Materials Science **46**, 559-632 (2001).

[2] P. Lichý, T. Elbel, I. Kroupová, F. Radkovský, Preparation and evaluation of properties of cast metallic foams with regular inner structure. Archives of Metallurgy and Materials **42**, 3, 1643-1646 (2017).

[3] T. Blejchař, Návody do cvičení "Modelování proudění" – CFX. 1. vyd. Ostrava: VŠB-TU, 133, 2009. ISBN 978-80-248-2050-7 URL: <http://www.338.vsb.cz/PDF/Blejchar-CFX.pdf>

[4] T. Blejchař, Turbulence Modelování proudění – CFX, učební texty. 1. vyd. Ostrava: VŠB-TU, 259, 2010. URL: <http://www.338.vsb.cz/PDF/Turbulence_ESF_v4.pdf>

[5] P. Cohen, K. Kundu, Fluid mechanics. Academic Press, 2004. ISBN: 978-0-12-178253-5

[6] J.Y. Tu, G.H Yeoh, C.Q. Liu, Computational Fluid Dynamics – A Practical Approach, Elsevier Science Limited, UK, 2008. ISBN: 978-0-7506-8563-4

[7] F. Radkovsky et al. Production of cast metal foams with a regular internal structure. In: 25th International Conference on Metallurgy and Materials Metal 2016, May 25th-27th 2016, Brno, Czech Republic. Brno: Tanger Ltd., Ostrava, 2015

[8] Z. Kadlec,Termomechanika, návody do cvičení. 1. vyd. Ostrava: VŠB-TU, 97, 2002. ISBN:978-80-248-1736-1